ESTIMATION OF LEVEE FAILURE POINTS BASED ON LEVEE VULNERABILITY INDEX AND FLOOD RISK ANALYSIS BY INTEGRATING SIMULATION OF FLOOD FLOW AND INUNDATION

KOSUKE TABATA & SHOJI FUKUOKA
Research Development Initiative, Chuo University, Japan

ABSTRACT

To examine the flood risk management measures, it is important to estimate the levee breach points, inundation discharge hydrograph and motion of the inundation water in the basin as precisely as possible. The purpose of this paper is to conduct the above series of studies on the Kinu River (Japan) suffered from inundation in the range of 40 km^2 due to overflowing and levee breach during the 2015 large flood. First, a simulation model integrating flood flow and inundation is developed. The inundation discharge hydrographs due to the overflowing and levee breach are estimated by the flood flow analysis based on observed temporal changes in water surface profiles in the Kinu River. The inundation is calculated by a two-dimensional model. The mesh of the inundation analysis model is generated by regular grid with 5 m size in order to express the microtopography obtained by DSM (Digital Surface Model). Manning's roughness coefficients are given according to the situation of the land use and inundation depth. It is confirmed that the developed model is useful by the inundation arrival time read from camera images and the spread of the actual inundation water in the basin. Next, the suitability of the levee vulnerability index t^* which has been derived by the authors is examined for the levees of the Kinu River. Finally, the inundation flow analysis is conducted under the actual and hypothetical levee breach conditions based on the value of t^*. It is concluded that the difference in the location and time of the levee breach influences on the motion of the inundation water and inundation areas in the Kinu River basin.

Keywords: Kinu River 2015 flood, inundation flow, flood flow, levee vulnerability index, flood risk.

1 INTRODUCTION

It is important to estimate the levee breach points, inundation discharge hydrograph and motion of the inundation water in the basin as precisely as possible to examine the flood risk management measures.

Tabata et al. [1] developed a flood flow analysis model based on the temporary changes of observed water surface profiles during the 2015 flood in the Kinu River, Japan, which suffered from damage in the huge inundation area due to levee breach. The inundation discharge hydrographs were estimated accurately by the developed flood flow model. Also, in the Joso City which faces the left bank of the Kinu River and inundated in the 2015 flood, the inundation time and depth were obtained from camera images installed at some locations in the Kinu River basin. These data will make it possible to verify the inundation analysis model.

In general flood risk assessment [2], levee breach points are usually set up at levee failure points where the water level exceeds the design water level. However, serious levee damage such as a levee breach and sliding or collapse has occurred at points where the body of the levee is vulnerable to seepage flow even in the section where the water level is below the design water level. In recent years, Fukuoka and Tabata [3] have proposed the levee vulnerable index t^* which is represented by the combination of water level, duration time of flood, levee width, porosity and permeability of the levee. It has been confirmed

WIT Transactions on Ecology and the Environment, Vol 234, © 2019 WIT Press
www.witpress.com, ISSN 1743-3541 (on-line)
doi:10.2495/RBM190081

that the levee vulnerability index can represent the risk of levee failure due to seepage flow. By using this index, the levee breach points will be estimated rationally.

The purpose of this paper is to estimate the flood risk by integrating simulation of flood flow and inundation in the Kinu River basin. First, the inundation flow analysis model is developed by using the inundation discharge hydrographs due to the overflowing and levee breach. Then, the inundation model is verified by the filed inundation data. Next, the levee failure risk due to seepage flow in the Kinu River is evaluated by the use of the levee vulnerability index t^*. Finally, the inundation flow analysis is conducted under the levee breach condition based on the value of t^*. It is concluded that the difference in the location and time of the levee breach considerably influences on the motion of the inundation water and inundation area in the Kinu River basin.

2 DEVELOPING THE INTEGRATING SIMULATION MODEL OF FLOOD FLOW AND INUNDATION

2.1 Integrated simulation model of flood flow and inundation in the Kinu River

Fukuoka and Watanabe [4] have proposed the numerical method for flood flows and bed variations using time series of observed flood water surface profiles on the basis of the idea that effects such as plan forms, cross-sections and outflowing water from the river appear in time series of observed water surface profiles of flood flows. Based on this idea, the integrated simulation model of flood flow and inundation was developed by using time series of the observed water surface profiles during the 2015 flood in the Kinu River [1]. Since overflowing and collapse of the levee occurred around 25.35 k, the inundation flow was calculated so that the collapse occurred when the water level exceeded the levee height. Also, the inundation flow from the levee breach point at 21.0 k was calculated so that the calculated water surface profiles agreed with the observed ones around the levee breached point [5] considering observed breach time and temporary change of breach width (Fig. 1). This model could not only elucidate the flood propagation in the Kinu River but also estimate inundation discharge hydrographs due to the overflowing and levee breach.

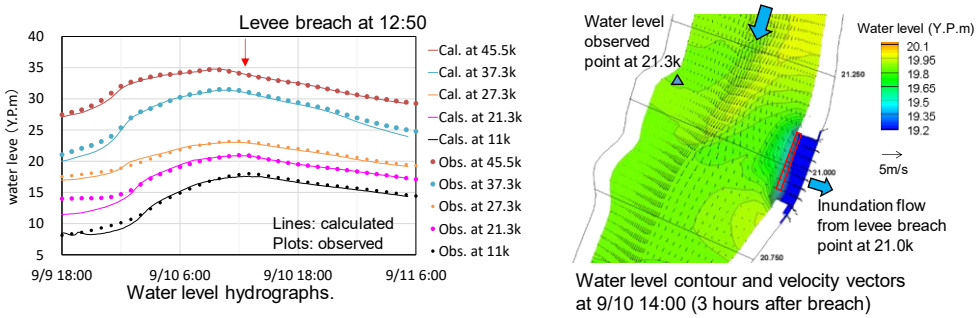

Figure 1: Calculated water level and inundation flows in the levee breach point at 21.0 k.

Fig. 2 shows the inundation discharge hydrographs which were estimated by this model. The first wave was caused by overflowing and collapse of levee around 25.35 k, which started at 06:00 on 10 September 2015, and the second one was caused by the levee breach at the 21 k left bank at 12:50 on 10 September 2015. The calculated inundation discharge

exceeded 500 m^3/s at the maximum and the volume was estimated to be 32,000,000 m^3. The measured total inundation volume was about 38,000,000 m^3, which agreed well with the computed result. The inundation flow analysis is carried out by using these inundation discharge hydrographs as the boundary conditions.

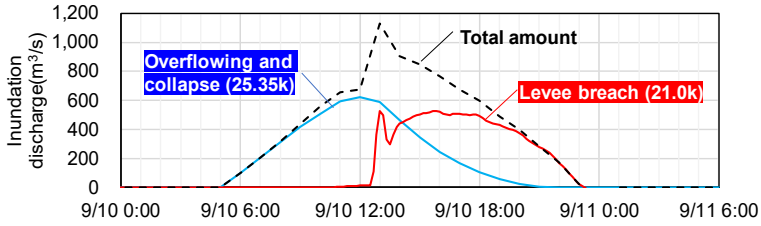

Figure 2: Estimated inundation discharge during the 2015 flood event in the Kinu River.

2.2 Inundation flow analysis in Joso City

A two-dimensional inundation analysis model for Joso City which faces the left bank levee in the Kinu River is developed by using the inundation discharge during the 2015 flood estimated by the analysis model in Section 2.1.

Fig. 3 shows the developed model for inundation analysis model in Joso City. The mesh is generated by regular grid with 5 m size in order to express the microtopography obtained by DSM (Digital Surface Model). Also, the mean ground level of each mesh is given by DSM. The land use classifications were set based on GIS data of farmlands, road networks and water area published by the Geophysical Survey Institute of Japan, and they were given to each mesh. Manning's roughness coefficients are given according to the land use and inundation depth. The roughness coefficients of farmland and water areas are given as 0.070 and 0.020 respectively. The roughness of the road is given small as 0.025 since it is generally known that the inundation water flows with high velocity on the road [6]. A large resistance acts on the inundation front flowing into the dry area, and the resistance is reduced at the place where was wet once. Therefore, a depth threshold h_0 (1.0 m in this study) related to dry or wet state is introduced. If the water depth is less than h_0 or has never been flooded, the roughness coefficient is given as 0.100, otherwise the one for each land use is given.

Fig. 4 shows a comparison between the observation and calculation of the temporal changes of the inundation depth at observed points St.1 and 2 in Fig. 1. The observed data were read from camera images at St.1 and 2. It can be confirmed that the inundation starts immediately after the levee breach at St.1. Also, the calculated data can roughly explain the observed one at St.2 which is far from the site of overflowing and levee breach. Therefore, it is shown that the developed model can express the spread of the inundation water from the Kinu River and the distribution of inundation water depth in Joso City.

Fig. 4 shows the inundation depth contours at 15:00 on 10 September and 0:00 on 11 September. First, part of the inundation water around 25.35 k flows into the main drainage channel and reaches the downstream part via the channel. At this time, the inundation water due to the levee breach at 21.0 k left bank was combined with the inundation water due to overflowing and collapse around 25.35 k. Also, the main body of the inundation water reached near the Joso City hall at 0:00 on 11 September (Fig. 4(b)), and a large-scale inundation occurred around the Joso City hall.

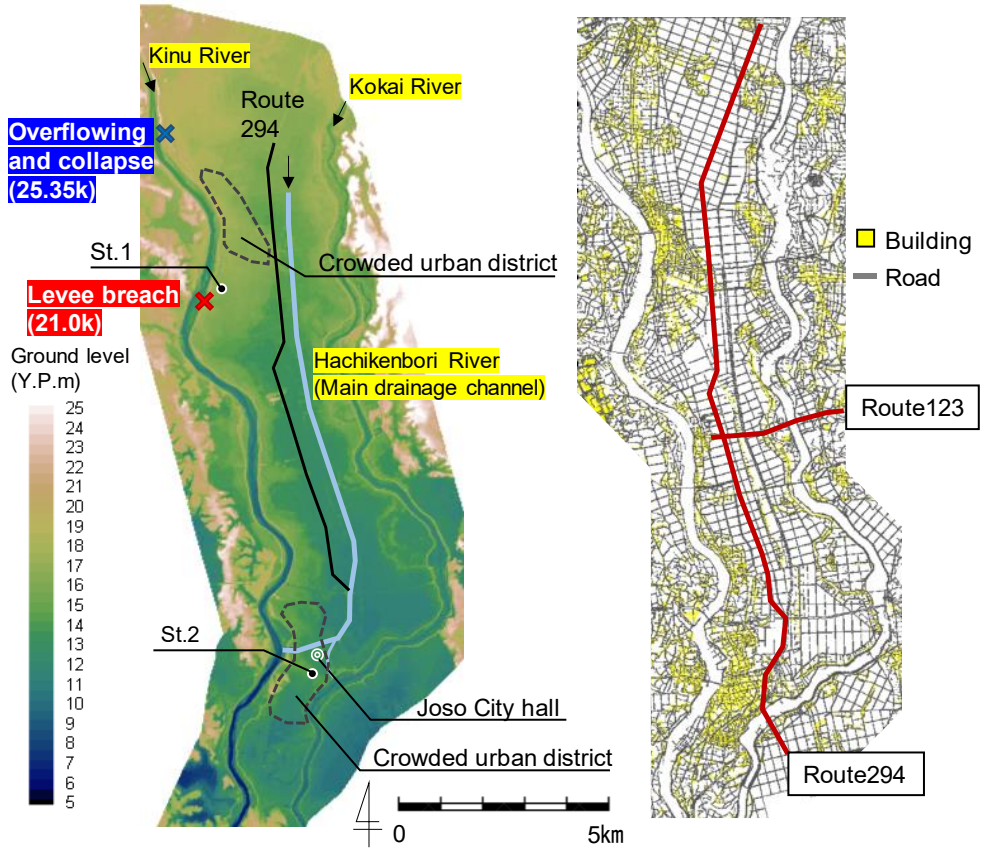

Figure 3: Developed inundation analysis model in Joso City.

3 EVALUATION OF LEVEE FAILURE RISK AND LEVEE BREACH POINTS BASED ON LEVEE VULNERABILITY INDEX

3.1 Levee vulnerability index t^* by the seepage flow

Fukuoka and Tabata [3] have proposed the dimensionless index for the levee failure due to seepage flow during a flood event; levee vulnerability index t^* (eqn (1)).

$$t^* = \frac{5}{2}\frac{kHt'}{\lambda b^2}. \tag{1}$$

Here, H is water level, b is horizontal length from the water front of waterside levee to the toe of the landside levee, t' is duration time from when the flood water level exceeds the ground level of the landside toe. k, λ and S_r are averaged permeability, porosity and degree of saturation of the levee, respectively (see Fig. 5(a)).

The levee vulnerability index t^* has been applied to many field levees where the damage had occurred, and it has become clear that when the value of t^* exceeds 0.1, the risk of levee breach due to the seepage flow tends to increase [3].

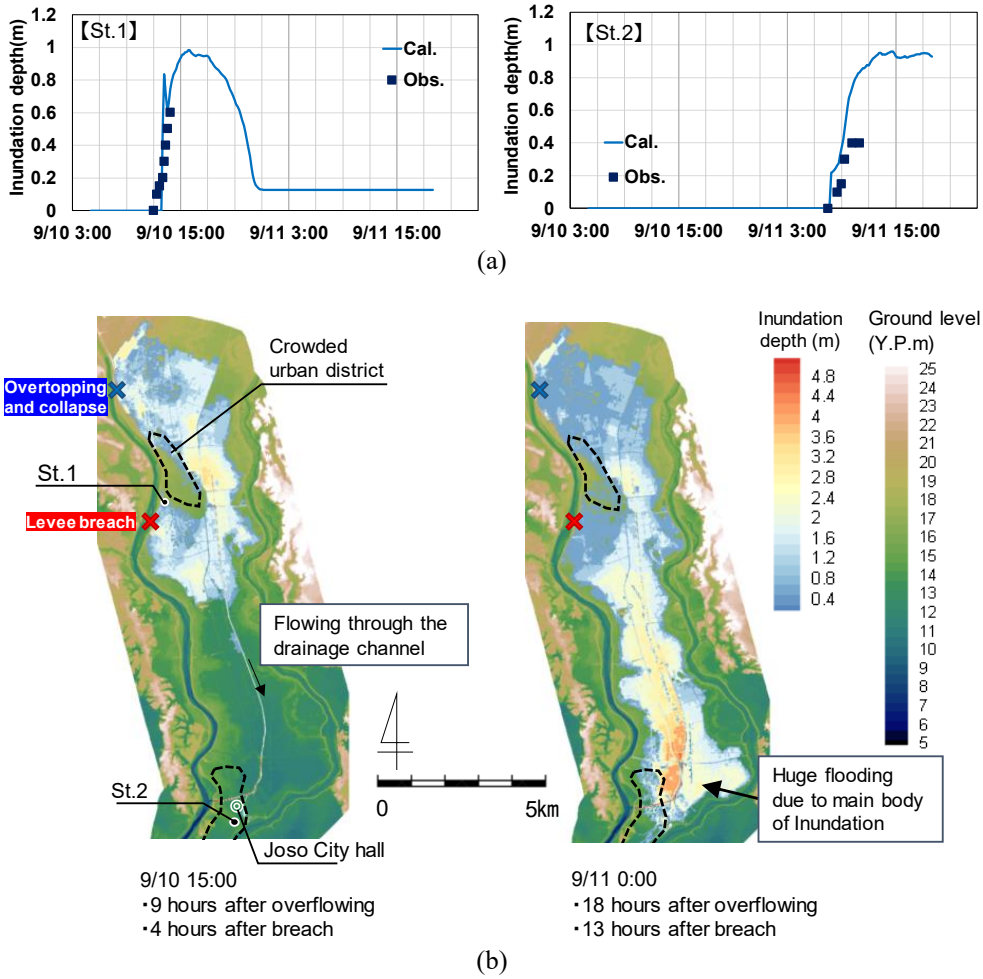

Figure 4: Inundation depth distribution in the Kinu River basin. (a) Comparison between calculation and observation at St.1 and St.2; and (b) Calculated inundation depth contour.

When the water level recedes, the top of the seepage line in the levee gradually moves to the landside toe. Therefore, the seepage flow from the top of the seepage line to the landside toe of the levee keeps on going and maintaining a high risk of levee failure. This is mainly caused by the reduction of the horizontal length b in eqn (1) due to the shift of the seepage peak height. Uemura and Fukuoka [7] have proposed the analysis method that can accurately represent the above-mentioned unsteady seepage phenomenon during the flood water receding stage. The outline of this method is shown below.

Consider the continuity condition that the volume change of water in the levee $\lambda \delta V$ coincides with the displacement $q\delta t$ from the body of the levee to the waterside due to the water level receding (see Fig. 5(b)).

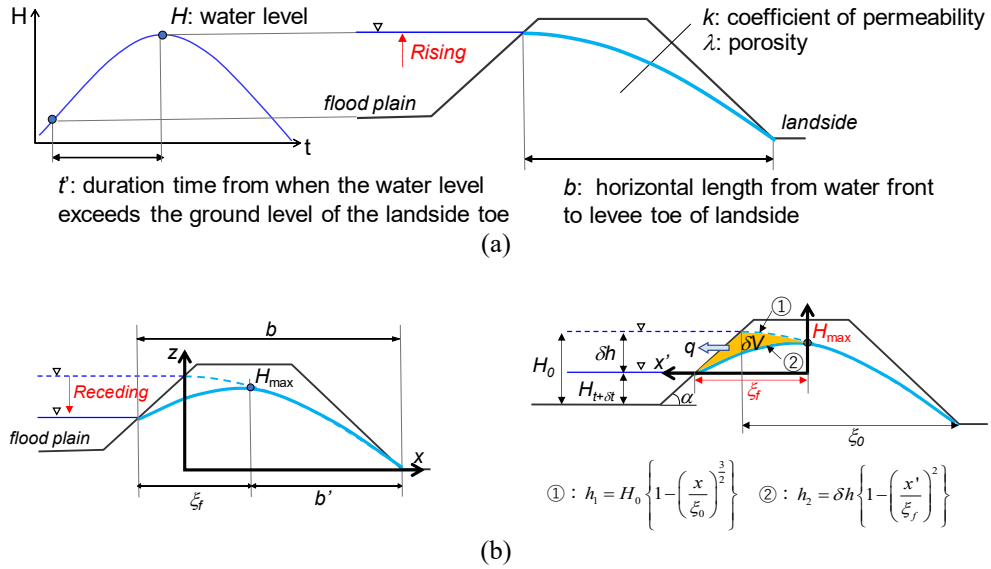

Figure 5: Definition of variables of levee vulnerability index t^*. (a) During water level rising (definition of variables in eqn (1)); and (b) During water level receding (definition of variables in eqns (2)–(5)) [7].

$$\lambda \delta V = q \delta t \,. \tag{2}$$

Here, δt is seepage time, δV is volume change of water in the levee per δt, q is outgoing discharge from waterside slope of the levee as the water level of rivers recedes. The left side of eqn (2) is indicated by the orange hatched area in Fig. 5(b) and expressed as eqn (3).

$$\begin{aligned} \lambda \delta V = {} & \frac{\lambda \delta h^2}{2\tan\alpha} - \frac{2}{3}\lambda \xi_f \left\{ \delta h - (\delta h + H_{t+\delta t}) \left(\frac{-\xi_f + \delta h / \tan\alpha}{-\xi_0} \right)^{3/2} \right\} \\ & -\lambda \left(-\xi_f + \frac{\delta h}{\tan\alpha} \right) \left\{ \frac{2}{5} (\delta h + H_{t+\delta t}) \left(\frac{-\xi_f + \delta h / \tan\alpha}{-\xi_0} \right)^{3/2} - \delta h \right\}. \end{aligned} \tag{3}$$

The right side of eqn (2) is expressed as eqn (4) by using Depuit–Forchheimer's equation [8]

$$q \delta t = \frac{k}{2\xi_f} \left[\left[H_0 \left\{ 1 - \left(\frac{-\xi_f + \delta h / \tan\alpha}{-\xi_0} \right)^{3/2} \right\} \right]^2 - H_{t+\delta t}^2 \right] * \delta t \,. \tag{4}$$

The horizontal position of seepage line's top ξ_f (see Fig. 5(b)) can be numerically solved since eqn (3) is equal to eqn (4). Then, the peak height of the seepage line's top H_{max} will be found by assuming that the position of the peak of the water level shifts along the seepage line. Therefore, the levee vulnerability index during the water level receding stage is expressed as eqn (5) by substituting H_{max} and b' (=b-ξ_f) for H and b in eqn (1)

$$t^* = \frac{5}{2}\frac{kH_{\max}t'}{\lambda b'^2}. \tag{5}$$

3.2 Calculated levee vulnerability index t^* and estimating of levee breach points

The levee vulnerability index t^* was calculated longitudinally for the Kinu River's left bank which faces Joso City. Fig. 6 shows the longitudinal distribution of the levee vulnerability index t^* at peak water level (black plots) and the maximum value of t^* during the water level receding stage (red plots). t^* around the actual breach point (21.0 k) are plotted in the range of 0.1 to 1.0 where the levee breach risk is very high. Besides these, t^* around 11.75 k exceed 0.1. Therefore, if the levee breach did not occur at 21.0 k, it might have occurred around 11.75k.

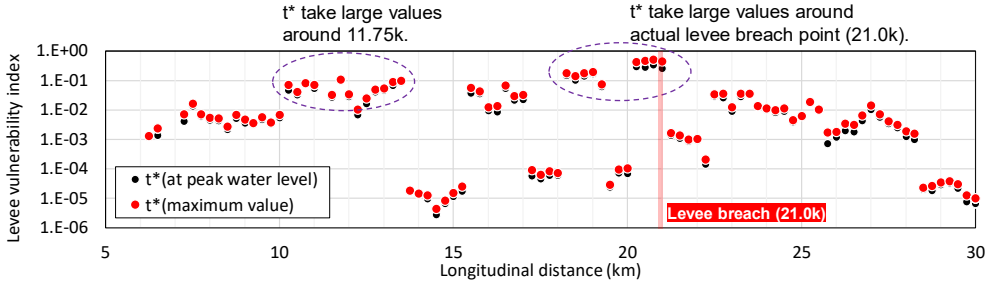

Figure 6: Longitudinal distribution of t^* along the left bank of the Kinu River.

Fig. 7 shows the temporary change of the water level and levee vulnerability index at 21 k and 11.75 k. It is confirmed that t^* exceeds 0.1 around the actual levee breach time (12:50 on 10 September) at 21 k left bank. Assuming that the levee breach occurs when t^* exceeds 0.1, the levee breach time at 11.75 k can be estimated as 17:00 on 10th September which is two hours after the peak water level.

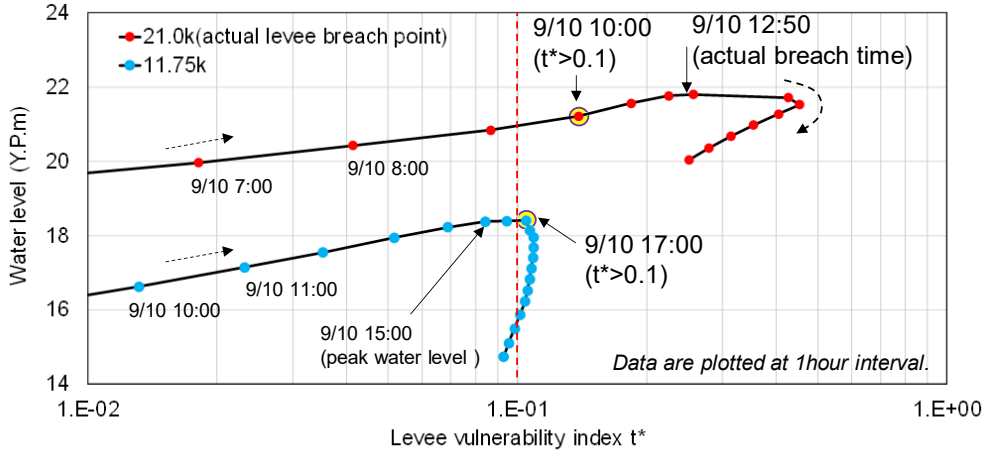

Figure 7: Temporary changes of water level and t^* at 21.0 and 11.75 k.

4 INUNDATION ANALYSIS UNDER A LEVEE BREACH SCENARIO BASED ON LEVEE VULNERABILITY INDEX

We need to conduct the inundation analysis under levee breach scenarios different from the actual flood inundation stated in Section 2.2 to investigate the inundation risk in the basin. In this section, the inundation discharge hydrograph is estimated, and the inundation analysis is performed under a hypothetical levee breach condition based on the result of the levee vulnerability index.

The hypothetical levee breach point was set at 11.75 k left bank in which t^* value took the second largest value after the actual levee bleach point at 21.0 k (see Fig. 6). Also, the levee breach time was set at 17:00 on 10 September when t^* exceeds 0.1 (see Fig. 7). This analysis was not taking account into the overflowing and collapse around 25.35 k. Fig. 8 shows the inundation discharge hydrograph due to the levee breach at 11.75 k left bank estimated by the simulation integrating the flood flow and inundation. The inundation discharge becomes about 500 m^3/s as well as the actual breach point at 21.0 k. However, since the levee breaches during the flood receding stage, the inundation volume is 7,500,000 m^3, which is smaller than the actual one.

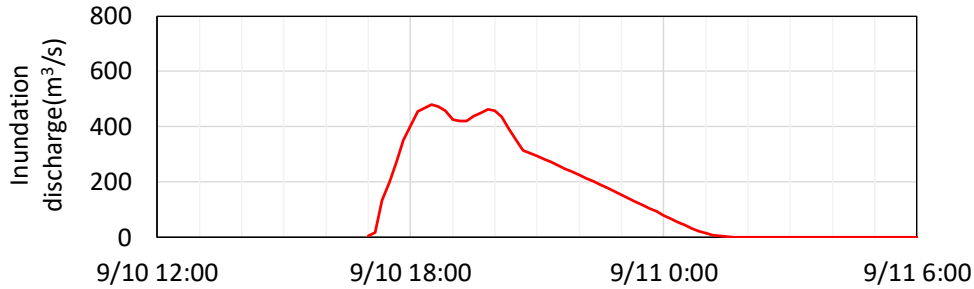

Figure 8: Estimated inundation discharge hydrograph due to the levee breach at 11.75 k.

The inundation flow analysis for the hypothetical levee breach condition at 11.75 k left bank based on the value of t^* was conducted. Fig. 9 shows the time change of the inundation depth contour. Although the inundation area is smaller than the actual one (Fig. 4), the inundation water spreads rapidly because the levee breach point is close to the crowded urban district of Joso City. It is shown that the maximum inundation depth in the crowded urban district (black dashed circle in Fig. 9) rises over 2.5 m, 4 hours after the levee breach at 11.75 k. Then, much of the inundation water flows northward on the west side of the main drainage channel. 12 hours after the levee breach, inundation water also spreads widely to the east of the main drainage channel. It is clear the crowded urban district of Joso City would suffer from the comparable large flood damage even if either 21k or 11.75k levee breached.

5 CONCLUSION

The integral simulation model for flood flow and inundation in the Kinu River basin suffered from inundation due to the levee breach at 21.0 k and overflowing and collapse around 25.35 k during the 2015 large flood was developed. This model can approximately elucidate the inundation arrival time read from camera images and the actual inundation water spread in the basin.

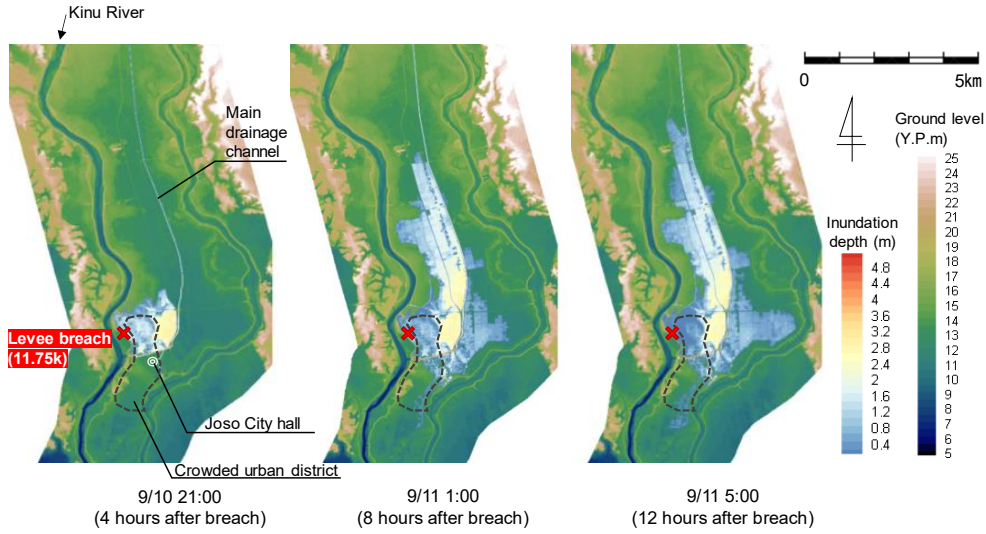

Figure 9: Inundation depth contour which is calculated taking account into the levee breach at 11.75 k left bank in the Kinu River.

Also, the levee vulnerability index t^* was calculated along the levee in the Kinu River and took high values at not only the actual levee breach point in 21.0 k but also 11.75 k.

The hypothetical inundation flow analysis by assuming that the levee breach occurs at 11.75 k was conducted. It is clear that the south crowded urban district of Joso City would suffer from the comparable huge flood damage even if either 21 k or 11.75 k levee breached. Therefore, the levee reinforcement against the seepage flow is needed at the places where the levee vulnerability index t^* take high values. It is expected to make an advanced inundation hazard map by performing the inundation flow analysis under the several levee breach scenarios based on the levee vulnerability index t^*.

REFERENCES

[1] Tabata, K., Fukuoka, S. & Deguchi, K., Analysis of discharge capacity and flood storage rate during 2015 large flood in the Kinu River. *12th International Conference on Hydro-Science and Engineering for Environmental Resilience, ICHE 2016*, 15-0036, 2016.

[2] Bilal, M., Jerry, F. & William, L., Risk analysis of a protected hurricane-prone region. I: model development. *Natural Hazards Review*, **10**(2), pp. 38–53, 2009.

[3] Fukuoka, S. & Tabata, K., Index governing the seepage flow and dynamic similarity condition of levee failure due to seepage flow: Seepage flow number and levee vulnerability index. *Annual Journal of Hydraulic Engineering, JSCE*, **74**(5), pp. I_1435–1440, 2018. (In Japanese.)

[4] Fukuoka, S. & Watanabe, A., Estimating Channel Storage and Discharge Hydrographs of Flooding. *Proceedings of the 5th International Conference on Hydro-Science and Engineering*, 2002.

[5] Fukuoka, S., Abe, T. & Tsukamoto, Y., Calculation method of inundation discharge hydrograph from the temporal changes in water surface profile due to levee breach. *Journal of JSCE*, **65**(3), pp. 166–178, 2009. (In Japanese.)

[6] Fukuoka, S., Kawashima, M., Matsunaga, N. & Maeuchi, H., Flooding water over a crowded urban district. *Journal of JSCE*, **491**(II-27), pp. 51–60, 1994. (In Japanese.)
[7] Uemura, Y. & Fukuoka, S., On the backslope stability of levee during the flood falling stage based on the levee vulnerability index. *Advances in River Engineering*, **24**, pp. 571–576, 2018. (In Japanese.)
[8] Muskat, M., *The Flow of Homogeneous Fluid through Porous Media*, McGraw-Hill, pp. 316, 1937.